Isocyanide Adducts of Tri- and Tetravalent Uranium Metallocenes Supported by Tetra(isopropyl)cyclopentadienyl Ligands

Journal:	*Dalton Transactions*
Manuscript ID	DT-ART-06-2020-002005.R2
Article Type:	Paper
Date Submitted by the Author:	04-Aug-2020
Complete List of Authors:	Boreen, Michael; University of California, Department of Chemistry Gross, Oliver; Paderborn University, Chemistry Department Hohloch, Stephan; Paderborn University, Chemistry Department Arnold, John; University of California, Department of Chemistry

Isocyanide Adducts of Tri- and Tetravalent Uranium Metallocenes Supported by Tetra(isopropyl)cyclopentadienyl Ligands†

Michael A. Boreen,[a,b] Oliver A. Groß,[c] Stephan Hohloch,[d,*] and John Arnold[a,b,*]

[a]*Department of Chemistry, University of California, Berkeley, California 94720, USA*
[b]*Chemical Sciences Division, Lawrence Berkeley National Laboratory, Berkeley, California 94720, USA*
[c]*Paderborn University, Warburger Straße 100, 33098 Paderborn, Germany*
[d]*University of Innsbruck, Faculty of Chemistry and Pharmacy, Institute of General, Inorganic and Theoretical Chemistry, Innrain 80-82, 6020 Innsbruck, Austria.*

Abstract

Reaction of the uranium(III) metallocenium salt $[(Cp^{iPr4})_2U][B(C_6F_5)_4]$ with *tert*-butyl isocyanide (^{t}BuNC) yielded the dicationic uranium(IV) complex $[(Cp^{iPr4})_2U(CN^tBu)_4][B(C_6F_5)_4]_2$ (**1**), which displays a linear metallocene geometry. Use of crude mixtures of $[(Cp^{iPr4})_2U][B(C_6F_5)_4]$, which contain a soluble source of iodide, led instead to isolation of the monocationic uranium(IV) iodide complex $[(Cp^{iPr4})_2U(I)(CN^tBu)_2][B(C_6F_5)_4]$ (**2**). Adduct formation with no change in oxidation state was observed upon addition of ^{t}BuNC to the neutral uranium(III) species $(Cp^{iPr4})_2UI$, resulting in isolation of $(Cp^{iPr4})_2U(I)(CN^tBu)$ (**3**). X-ray crystallographic and IR spectroscopic studies both showed effects ascribed to the presence of multiple strongly donating isocyanide ligands in **1**.

Introduction

The chemistry of trivalent uranium has developed rapidly in the past few decades as new synthetic routes have provided facile access to uranium(III) starting materials.[1–7] Much of the interest in this oxidation state of uranium stems from its ability to act as a potent reductant for a variety of transformations with small molecules.[1,8–11] Given the fundamental importance of metallocene chemistry to the development of actinide chemistry,[12–14] the uranium(III) metallocenium species $[(C_5Me_4R)_2U][(\mu\text{-}Ph)_2BPh_2]$ (R = H, Me, $SiMe_3$) containing coordinated BPh_4^- anions represent an important class of low-valent uranium synthons.[15–17] The redox and ligand substitution reactivity of these species continues to be the focus of many studies.[15,17–27]

Recently, the first base-free uranium(III) metallocenium cations $[(Cp^{iPr5})_2U][B(C_6F_5)_4]$ and $[(Cp^{iPr4})_2U][B(C_6F_5)_4]$ ($Cp^{iPr5} = C_5(^iPr)_5$, $Cp^{iPr4} = C_5(^iPr)_4H$) were reported.[28,29] To-date, the reactivity of these species is minimal, amounting to coordination of 1,2-dimethoxyethane (DME) to $[(Cp^{iPr4})_2U][B(C_6F_5)_4]$ to form the Lewis adduct $[(Cp^{iPr4})_2U(DME)][B(C_6F_5)_4]$.[29] As a part of our continuing studies using the $(Cp^{iPr4})_2U$ fragment with both uranium(III) and uranium(IV),[29–31] we sought to expand the reactivity of the $[(Cp^{iPr4})_2U]^+$ cation.

Previous studies have used nitriles to generate cationic actinide metallocenium species, including rare examples of linear actinide metallocenes,[32–34] but, compared to nitriles, the reactivity of isonitriles with actinide complexes has been the subject of significantly fewer studies. Here, we describe the behavior of $[(Cp^{iPr4})_2U][B(C_6F_5)_4]$ toward *tert*-butyl isocyanide (^tBuNC), which, in contrast to reactions with DME, produced exclusively tetravalent complexes, including a linear, dicationic metallocenium species. Intriguingly, we observed different products from the reaction between the metallocenium complex and ^tBuNC depending on whether or not an iodide source was present.

Results and Discussion

Addition of excess ^tBuNC to a diethyl ether solution of hexane-washed crude $[(Cp^{iPr4})_2U][B(C_6F_5)_4]$ led to rapid precipitation of orange-brown crystalline material identified as $[(Cp^{iPr4})_2U(CN^tBu)_4][B(C_6F_5)_4]_2$ (**1**), a dicationic complex containing four isocyanide ligands and two coplanar cyclopentadienyl units (Scheme 1). Complex **1** was isolated after work-up in 40%

yield based on $[(Et_3Si)_2(\mu\text{-H})][B(C_6F_5)_4]$ as the limiting reagent (since the product contains two $[B(C_6F_5)_4]^-$ ions per uranium center). In generating **1** from $[(Cp^{iPr4})_2U][B(C_6F_5)_4]$, the uranium center became oxidized by one electron to uranium(IV). In an attempt to explore the mechanism of this process, volatile components of the reaction mixture were collected for GC/MS analysis (see ESI); however, apart from small amounts of ^{t}BuNC and Et_3SiH, no reduction products from this reaction were detected.[#]

Scheme 1. Syntheses of complexes **1**, **2**, and **3**.

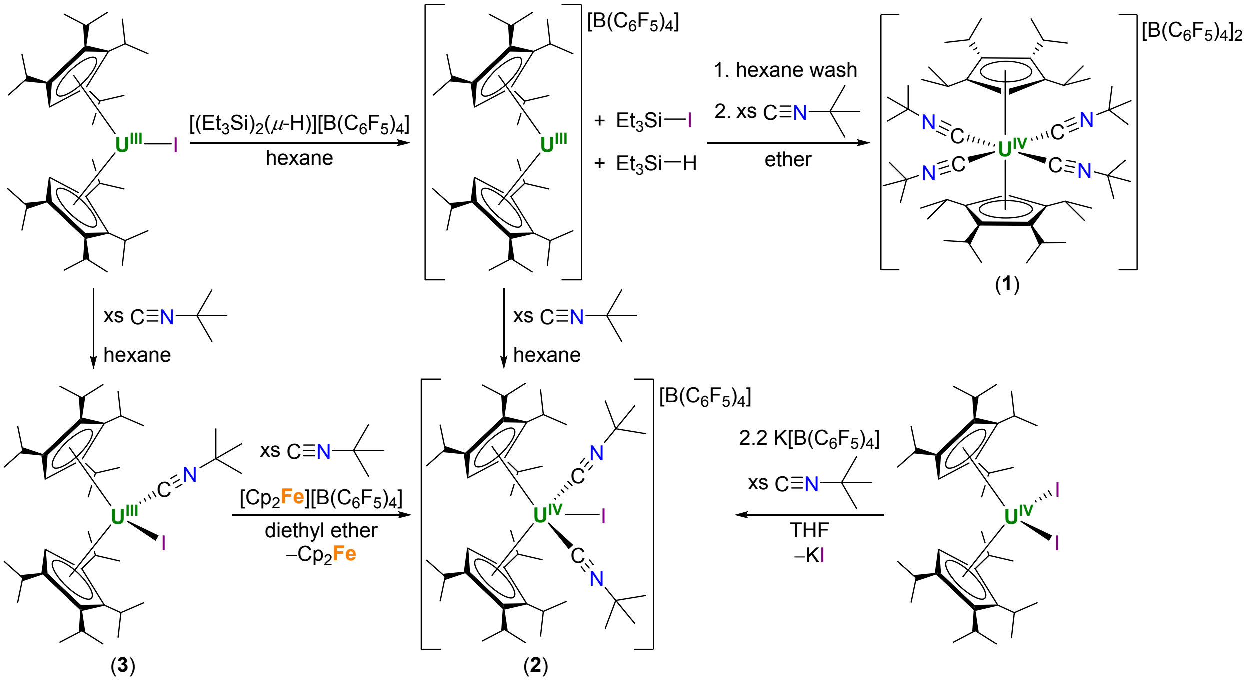

Interestingly, upon further attempts to explore the mechanism of oxidation, a different reaction outcome was observed when byproducts from the halide abstraction to form $[(Cp^{iPr4})_2U][B(C_6F_5)_4]$ were still present. The metallocene salt starting material is formed by iodide abstraction from $(Cp^{iPr4})_2UI$ using $[(Et_3Si)_2(\mu\text{-H})][B(C_6F_5)_4]$, a process that generates the byproducts Et_3SiI and Et_3SiH.[29,35] Addition of excess ^{t}BuNC to crude mixtures of

$[(Cp^{iPr4})_2U][B(C_6F_5)_4]$ that were not washed with hexane led to isolation of dark red crystals of $[(Cp^{iPr4})_2U(I)(CN^{t}Bu)_2][B(C_6F_5)_4]$ (**2**) in 23% yield after crystallization from diethyl ether. As observed in the formation of **1**, the uranium center in **2** became oxidized to uranium(IV) during the course of the reaction. However, **2** is monocationic, with the increase of metal charge compensated by the abstraction of an iodide ion, presumably from the equivalent of Et_3SiI remaining in solution.‡

Seeking higher yielding, more rational syntheses of **1** and **2**, we attempted to prepare **2** via isocyanide addition to $(Cp^{iPr4})_2UI$ followed by oxidation. Addition of excess ^{t}BuNC to hydrocarbon solutions of $(Cp^{iPr4})_2UI$ caused a rapid color change from dark blue to dark yellow-green. The neutral mono-adduct $(Cp^{iPr4})_2U(I)(CN^{t}Bu)$ (**3**) was isolated as a green crystalline solid after crystallization from pentane in 85% yield. Oxidation of *in situ* generated **3** with $[Cp_2Fe][B(C_6F_5)_4]$ in the presence of excess ^{t}BuNC enabled isolation of **2** in higher yield (49%, compared to 23% via crude $[(Cp^{iPr4})_2U][B(C_6F_5)_4]$). Additionally, we assumed that starting from the uranium(IV) complex $(Cp^{iPr4})_2UI_2$, salt metathesis of either one or both of the iodide ions with $[B(C_6F_5)_4]^{-}$ in the presence of excess ^{t}BuNC would generate **2** or **1**, respectively. In fact, we found that reaction between $(Cp^{iPr4})_2UI_2$, two equivalents of $K[B(C_6F_5)_4]$, and excess ^{t}BuNC in THF exclusively led to formation of **2** in 32% isolated yield.

Single crystal X-ray crystallography confirmed the solid-state structures of **1**, **2**, and **3** (Figure 1). Obtaining diffraction data of adequate quality for **1** proved challenging; a possible explanation for this difficulty can be proposed based on the nearly spherical shape of the $[(Cp^{iPr4})_2U(CN^{t}Bu)_4]^{2+}$ fragment: related bulky metallocene complexes are known to yield poorly-ordered structures due to resulting small energetic differences in crystal packing effects.[36] The large thermal ellipsoids for **1** compared to those of **2** and **3** are likely a result of disorder originating from such low preferences for specific orientations.

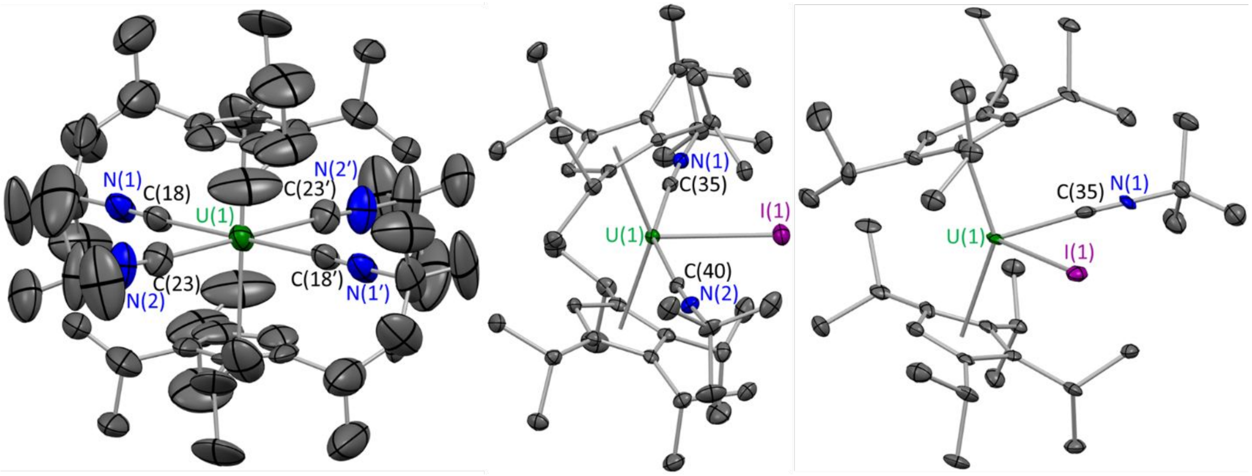

Figure 1. X-ray crystal structures of $[(\mathrm{Cp}^{\mathrm{iPr4}})_2\mathrm{U}(\mathrm{CN}^t\mathrm{Bu})_4][\mathrm{B}(\mathrm{C}_6\mathrm{F}_5)_4]_2$ (**1**, left), $[(\mathrm{Cp}^{\mathrm{iPr4}})_2\mathrm{U}(\mathrm{I})(\mathrm{CN}^t\mathrm{Bu})_2][\mathrm{B}(\mathrm{C}_6\mathrm{F}_5)_4]$ (**2**, middle), and $(\mathrm{Cp}^{\mathrm{iPr4}})_2\mathrm{U}(\mathrm{I})(\mathrm{CN}^t\mathrm{Bu})$ (**3**, right) with 50% probability ellipsoids. Hydrogen atoms and $[\mathrm{B}(\mathrm{C}_6\mathrm{F}_5)_4]^-$ counteranions are omitted for clarity. Selected structural metrics are listed in Table 1.

Focusing on the Cp(cent)–U–Cp(cent) angles, **2** and **3** display similar bent metallocene geometries with values of 142.19(5) and 143.0(1)°, respectively. However, in **1**, the $[(\mathrm{Cp}^{\mathrm{iPr4}})_2\mathrm{U}(\mathrm{CN}^t\mathrm{Bu})_4]^{2+}$ units crystallize in space group $P\bar{1}$ with the uranium atom on an inversion center, meaning a 180° Cp(cent)–U–Cp(cent) angle is crystallographically imposed. Linear actinide metallocenes are extremely rare but were first observed by Ephritikhine and coworkers in the uranium(IV) dicationic $[\mathrm{Cp}^*{}_2\mathrm{U}(\mathrm{NCMe})_5]^{2+}$ fragment.[32–34,37,38] In the linear metallocene uranium(IV) and thorium(IV) species $[\mathrm{Cp}^*{}_2\mathrm{U}(\mathrm{NCMe})_5]^{2+}$, $[\mathrm{Cp}^*{}_2\mathrm{U}(\mathrm{CN})_5]^{3-}$, and $[\mathrm{Cp}^*{}_2\mathrm{Th}(\mathrm{NCR})_5]^{2+}$ (R = Me, Ph), this geometry is promoted by saturation of the equatorial girdle with donor ligands,[32–34,37] as appears to be the case in **1** as well. However, a very different type of uranium metallocene, the neutral, divalent complex $(\mathrm{Cp}^{\mathrm{iPr5}})_2\mathrm{U}$, was recently isolated and also found to display a linear metallocene geometry.[38,§]

The U–I bond length in **3** is roughly 0.08 Å longer than that of **2**, roughly equivalent to the expected difference in effective ionic radii between the respective uranium centers (Table 1).[§§] In contrast, the average U–$\mathrm{C}_{\mathrm{isocyanide}}$ distance of **2** (2.599(4) Å) is essentially equivalent to the U–$\mathrm{C}_{\mathrm{isocyanide}}$ distance of 2.602(8) Å in **3**. Moreover, the average U–$\mathrm{C}_{\mathrm{isocyanide}}$ bond length of 2.643(8) Å in **1** is longer than those of **2** and **3** despite the higher charge state of the complex ion in **1**. Similarly, the U–Cp(cent) distance in **1** (2.565(3) Å) is longer than those of **2** and **3** (2.495(2) and 2.532(3) Å, respectively). These results are consistent with the explanation that strong donation from the isocyanide ligands significantly compensates for the buildup of positive charge on the uranium center that would otherwise be expected as oxidation state and complex ion charge increase (see discussion of ν_{NC} values below). Greater steric pressure from the presence of four ^{t}BuNC ligands in **1** also likely contributes to longer U–$\mathrm{C}_{\mathrm{isocyanide}}$ and U–Cp(cent) distances. The shorter average U–Cp(cent) distance in **2** versus in **3** is consistent with the higher oxidation state and complex ion positive charge in **2** with only one additional ^{t}BuNC not causing a large amount of steric pressure.

Table 1. Selected Distances (Å) and Angles (°) for **1**, **2** and **3**.

Complex	U–$\mathrm{C}_{\mathrm{isocyanide}}$	U–Cp(cent)	Cp(cent)–U–Cp(cent)	U–I
1	2.635(9), 2.650(7)	2.565(3)	180	—
2	2.584(4), 2.613(4)	2.494(2), 2.495(2)	142.19(5)	2.9903(4)
3	2.602(8)	2.518(3), 2.546(3)	143.0(1)	3.0691(6)

The IR spectra of **1**, **2**, and **3** each displayed a single strong, sharp ν_{NC} band at 2176, 2182, and 2166 cm^{-1}, respectively, all higher than the frequency for free ^{t}BuNC (2134 cm^{-1}).[39,40] An increase in ν_{NC} is typically observed for isocyanides upon coordination to electropositive metal ions that do not participate in significant π-backbonding interactions.[41–43] Nonetheless, uranium(III) complexes $(Cp^R)_3U$ (Cp^R = substituted cyclopentadienyl) have been shown to undergo back-donation to the isocyanide π* orbitals in their respective adducts, with ν_{NC} values of 2127 and 2140 cm^{-1} reported for $(C_5Me_4H)_3U(CN^tBu)$ and $(1,3\text{-}(Me_3Si)_2C_5H_3)_3U(CN^tBu)$, respectively, compared to a ν_{NC} value of 2178 cm^{-1} in $(1,3\text{-}(Me_3Si)_2C_5H_3)_3La(CN^tBu)$, in which no π-backbonding is expected.[43,44]

The ν_{NC} value of **3** (2166 cm^{-1}) is larger than the abovementioned $(Cp^R)_3U(CN^tBu)$ species as well as that of the uranium(III) complex $[Cp^*{}_2U(CN^tBu)(\mu\text{-}CN)]_3$ (2143 cm^{-1}),[45] suggesting minimal or insignificant π-backbonding in **3**. The uranium(IV) cation $[Cp^*{}_2U(NMe_2)(CN^tBu)_2][BPh_4]$ has a similar ν_{NC} value (2181 cm^{-1}) to that of closely related cation **2**,[46] while the neutral uranium(IV) and uranium(V) complexes $Cp^*{}_2U(CN^tBu)(\eta^2\text{-}N(^tBu)C{=}PPh)$ and $(Cp^*)(\eta^8\text{-}C_8H_6\text{-}1,4\text{-}(Si^iPr_3)_2)U(O)(CN^tBu)$ display ν_{NC} values of 2171 and 2179 cm^{-1}, respectively.[40,47] Although a higher ν_{NC} might be expected for dicationic **1** relative to **2** on the basis of complex ion charge, the increased number of strongly donating isocyanide ligands in **1** would be expected to have the opposite effect, and the different geometry of the Cp^{iPr4} ligands is a further complicating factor; the net result is a slightly lower ν_{NC} value in **1**.

In the ^{1}H NMR spectra of **1**, **2**, and **3**, a single peak corresponding to the *tert*-butyl groups of the isocyanide ligands was observed for each complex at −18.14, −16.30, and −12.84 ppm, respectively. For **2** and **3**, the ^{t}Bu resonance was relatively sharp (FWHM = 9.6 and 16 Hz, respectively), while the resonances for the Cp^{iPr4} ligands were very broad due to dynamic behavior discussed previously in related species (Figures S3 and S5).[29,31] For **1**, the ^{t}Bu resonance was broad (FWHM = 400 Hz), and the Cp^{iPr4} ligand resonances were too broad to be observed (Figure S1). Notably, traces of (Cp^{iPr4})$_2$UI$_2$ were observed in the ^{1}H NMR spectrum of **2**.

Cyclic voltammograms (CVs) of **1**, **2**, **3**, and (Cp^{iPr4})$_2$UI were recorded in THF using [^{n}Bu$_4$N][B(C$_6$F$_5$)$_4$] as the supporting electrolyte (see ESI for details). In contrast to the simple redox behavior of (Cp^{iPr4})$_2$UX$_2$ ($X^- = F^-, Cl^-, Br^-, I^-, N_3^-$, NCO$^-$) in which only one feature (the reversible uranium(III/IV) redox couple) was observed for each species[29,31], multiple features were observed for each of the complexes measured in this work. Further complicating electrochemical analysis, **2** decomposed significantly, and **1** decomposed completely, within several minutes under these electrochemical conditions.

Nevertheless, reductive features were observed for **1** and **2**: the $E_{1/2}$ value for the first reduction wave was measured at −0.68 and −1.00 V versus the ferrocene/ferrocenium (Fc/Fc$^+$) redox couple for **1** and **2**, respectively. Comparison to (Cp^{iPr4})$_2$UI$_2$, which displayed an $E_{1/2}$ value of −1.41 V vs Fc/Fc$^+$ for the uranium(III/IV) redox couple,[29] demonstrates that reduction of **1** and **2** should occur at more mild potentials than those necessary to reduce the related neutral (Cp^{iPr4})$_2$UX$_2$ species.

Two oxidative features ($E_{1/2} = -1.45$ and −1.03 V vs Fc/Fc$^+$) were observed for **3**, with the second feature more intense than the first. An overall similar profile was observed in CVs of (Cp^{iPr4})$_2$UI, although the return waves for the first two oxidation waves of (Cp^{iPr4})$_2$UI were split with relative intensities that varied with the scan rate (see Figures S15–S17). Previous work demonstrated that (Cp^{iPr4})$_2$UI reversibly binds THF in solution, but the nature of the solution-state ligand coordination-dissociation equilibria in **3** and (Cp^{iPr4})$_2$UI has not been fully characterized and likely has a strong influence on the observed CV data.

Conclusions

Addition of ^{t}BuNC to $[(Cp^{iPr4})_2U][B(C_6F_5)_4]$ produced uranium(IV) complexes as the only isolable products. When iodide sources present after generation of the metallocenium salt were washed away, the dicationic complex $[(Cp^{iPr4})_2U(CN^{t}Bu)_4][B(C_6F_5)_4]_2$ (**1**) was isolated. However, addition of ^{t}BuNC to crude $[(Cp^{iPr4})_2U][B(C_6F_5)_4]$ yielded the monocationic complex $[(Cp^{iPr4})_2U(I)(CN^{t}Bu)_2][B(C_6F_5)_4]$ (**2**). Addition of ^{t}BuNC to solutions of $(Cp^{iPr4})_2UI$ led to mono-adduct formation without a change in oxidation state, yielding $(Cp^{iPr4})_2U(I)(CN^{t}Bu)$ (**3**). X-ray crystallography and infrared spectroscopy revealed effects of having a large number of strongly donating isocyanide ligands in **1**, most notably resulting in a rare linear metallocene geometry.

Experimental Section

General Considerations: Unless otherwise noted, all reactions were performed using standard Schlenk line techniques under an atmosphere of nitrogen or argon or in an MBraun inert atmosphere glove box under an atmosphere of nitrogen. Glassware and Celite® were stored in an oven at *ca*. 150 °C for at least 3 h prior to use. Molecular sieves (4 Å) were activated by heating to 200 °C overnight under vacuum prior to storage in a glove box. NMR spectra were recorded at room temperature unless noted otherwise on Bruker AV-300, AVB-400, AVQ-400, AV-500, or AV-600 spectrometers. ^{1}H NMR chemical shifts (δ) are given relative to residual solvent peaks and are recorded in units of parts per million (ppm). Default (0.3 Hz) line broadening functions were applied to ^{1}H NMR spectra unless stated otherwise. Where peaks in the ^{1}H NMR spectra could be fitted, full width at half maximum (FWHM) values are reported in Hertz as determined by least squares fitting of data to Lorentzian line shapes in MestReNova (version 14.1.2-25024). ^{19}F NMR chemical shifts (δ) are reported in ppm and referenced to an external standard ($CFCl_3$ in

$CDCl_3$). FT-IR samples were prepared as Nujol mulls pressed between KBr plates, with data collected with a Nicolet iS10 FT-IR spectrometer. UV-visible measurements were performed on a Varian Cary® 50 UV-Vis Spectrophotometer. A two mm path length quartz cell was used, and a blank was subtracted from each run. GC/MS measurements were performed using an Agilent 5975C 7890A GC/MS System. Elemental analyses were determined at the Microanalytical Facility at the College of Chemistry, University of California, Berkeley.

Materials: Diethyl ether, *n*-hexane, *n*-pentane, and THF were purified by passage through columns of activated alumina and degassed by sparging with nitrogen. C_6D_6 and THF-d_8 were vacuum transferred from a flask containing sodium/benzophenone and stored over molecular sieves. $(Cp^{iPr4})_2UI$,[29] $(Cp^{iPr4})_2UI_2$,[29] and $[(Et_3Si)_2(\mu\text{-H})][B(C_6F_5)_4]$[35] were synthesized according to literature procedures. $[Cp_2Fe][B(C_6F_5)_4]$ was synthesized by using $K[B(C_6F_5)_4]$ in place of $[NH_4][PF_6]$ in the literature procedure for $[Cp_2Fe][PF_6]$.[48,49] $K[B(C_6F_5)_4]$ was generously donated by Boulder Scientific Company. All other chemicals were purchased from commercial sources and used as received.

$[(Cp^{iPr4})_2U(CN^tBu)_4][B(C_6F_5)_4]_2$ (1). Hexane (1.5 mL) was added to a mixture of $(Cp^{iPr4})_2UI$ (37 mg, 0.044 mmol, 1.0 equiv) and $[(Et_3Si)_2(\mu\text{-H})][B(C_6F_5)_4]$ (45 mg, 0.049 mmol, 1.0 equiv), and the resulting suspension was stirred vigorously for 1 h at room temperature. The solution was then decanted, and the blue solid was washed with 3 × 1 mL of hexane to remove any remaining Et_3SiI, Et_3SiH, and $(Cp^{iPr4})_2UI$. The crude $[(Cp^{iPr4})_2U][B(C_6F_5)_4]$ was extracted into 15 mL of diethyl ether and filtered through Celite to yield a dark blue solution. A solution of ^tBuNC (25 µL, 0.22 mmol, 5.0 equiv) in 1 mL of diethyl ether was added by pipette with stirring at room temperature, and the resulting mixture quickly turned orange and formed crystalline orange-brown precipitate. After stirring at room temperature for an additional 20 min, volatiles were removed *in vacuo*, and the product was extracted into 2 mL of THF, filtered through Celite, and dried again *in vacuo* to form a red oil. Diethyl ether (1.5 mL) was then added to the crude product, and the mixture was swirled for several seconds before sitting undisturbed at room temperature, causing the material to dissolve initially then rapidly form crystalline solid. The mixture was allowed to sit for an additional hour at room temperature then was cooled to −40 °C overnight. The product was isolated as brown microcrystalline solid by vacuum filtration over a fine-porosity fritted filter, washed with 3 × 2 mL of diethyl ether, and dried *in vacuo* (25 mg, 0.010 mmol, 43% yield (based on $[(Et_3Si)_2(\mu\text{-}H)][B(C_6F_5)_4]$ as the limiting reagent)). X-ray quality crystals of **1** were grown from diethyl ether/THF (~20:1 ratio) at room temperature. ^1H NMR (600 MHz, THF-d_8): δ −18.14 (s, FWHM = 400 Hz, $CNC(CH_3)_3$); no additional resonances were found within the range 100 to −100 ppm, presumably due to the extreme broadness of the signals corresponding to the Cp^{iPr4} ligands (see Figure S1); ^{19}F NMR (376 MHz, THF-d_8): δ −134.31 (m), −166.25 (t, $J = 20$ Hz), −169.87 (t, $J = 19$ Hz)); $\mu_{eff} = 3.35\ \mu_B$ (298 K, Evans method, THF-d_8); IR: 2176 (s, ν_{CN}), 1644 (s), 1514 (s), 1272 (m), 1236 (w), 1178 (s), 1088 (s), 977 (s), 861 (w), 774 (s), 756 (s), 684 (m), 662 (s), 608 (w), 603 (w), 574 (w), 527 (w). Anal. Calcd. (%) for $C_{102}H_{94}B_2F_{40}N_4U$ (**1**): C, 51.14; H, 3.96; N, 2.34. Found: C, 51.13; H, 4.04; N, 2.55.

$[(Cp^{iPr4})_2U(I)(CN^tBu)_2][B(C_6F_5)_4]$ (2). *Method A*. A solution of ^{t}BuNC (12 μL, 0.10 mmol, 2.2 equiv) in 1 mL of diethyl ether was added to a solution of $(Cp^{iPr4})_2UI$ (39 mg, 0.047 mmol, 1.0 equiv) in 1 mL of diethyl ether at room temperature with stirring. After stirring the resulting green solution for an additional minute, $[Cp_2Fe][B(C_6F_5)_4]$ (42 mg, 0.048 mmol, 1.0 equiv) was added to the reaction mixture as a solid with stirring, quickly resulting in a dark red suspension. The reaction mixture was stirred for an additional 20 min at room temperature, then volatiles were removed *in vacuo*. The crude solid was washed with 4 × 1 mL of hexane to remove Cp_2Fe and was dried again *in vacuo*. The product was extracted into 1 mL of THF and filtered through Celite. Hexane (2 mL) was layered on top, and the resulting mixture was allowed to sit undisturbed at −40 °C. The product was isolated as dark red crystals, washed with 1 mL of hexane, and dried *in vacuo* (38 mg, 0.023 mmol, 49% yield). X-ray quality crystals of **2** were grown from diethyl ether at room temperature. ^1H NMR (400 MHz, THF-d_8): δ 74.8 to 68.5, 46.2 to 39.0, 38.5 to 31.7, 30.6 to 24.3, 21.7 to 17.3, 13.6 to 8.2, 7.7 to 1.1 (this signal is particularly difficult to identify as it overlaps a considerably amount of the diamagnetic region), −16.30 (s, FWHM = 9.6 Hz, $CNC(CH_3)_3$), −32.1 to −38.3, −39.5 to −44.0, other signals could not be identified due to the intrinsic broad nature of the signals and the related difficulty of correcting the spectrum's baseline at room temperature; ^{19}F NMR (376 MHz, THF-d_8): δ −134.22 (m), −166.38 (t, J = 20 Hz), −169.92 (t, J = 19 Hz); $\mu_{eff} = 3.08\ \mu_B$ (298 K, Evans method, THF-d_8); IR: 2182 (s, ν_{CN}), 1643 (m), 1514 (s), 1276 (m), 1235 (w), 1183 (m), 1147 (w), 1087 (s), 1038 (w), 981 (s), 928 (w), 906 (w), 833(w), 799 (m), 774 (m), 769 (m), 756 (s), 685 (n), 661 (s), 610 (w), 603 (w), 573 (w), 552 (w), 539 (w), 525 (w). Anal. Calcd. (%) for $C_{68}H_{76}BF_{20}IN_2U$ (**2**): C, 48.70; H, 4.57; N, 1.67. Found: C, 48.87; H, 4.63; N, 1.80.

Method B. Hexane (1.5 mL) was added to a mixture of $(Cp^{iPr4})_2UI$ (30 mg, 0.036 mmol, 1.0 equiv) and $[(Et_3Si)_2(\mu\text{-}H)][B(C_6F_5)_4]$ (36 mg, 0.039 mmol, 1.1 equiv), and the resulting suspension was stirred vigorously for 4 h at room temperature. Dark blue solids rapidly precipitated, and the solution gradually changed from dark blue to dark yellow-green. Next, ^{t}BuNC (21 μL, 0.18 mmol, 5.0 equiv) was added to the reaction mixture by pipette, resulting in a rapid color change to an orange solution with concomitant formation of a red-orange oily solid. The suspension was stirred for an additional hour at room temperature, then the solution was decanted, and the oily solid was washed with 3 × 1 mL of hexane before drying *in vacuo*. The solid was extracted into 2 mL of diethyl ether, filtered through Celite, concentrated to a volume of 0.5 mL, and cooled to −40 °C. The product was isolated as dark red crystals, washed with 1 mL of hexane, and dried *in vacuo* (14 mg, 0.0082 mmol, 23% yield). The IR spectrum of **2** prepared by this method was identical to that isolated by Method A above.

Method C. A solution of ^{t}BuNC (16 μL, 0.14 mmol, 10 equiv) in 2 mL of THF was added by pipette to a dark red-orange solution of $(Cp^{iPr4})_2UI_2$ (14 mg, 0.014 mmol, 1.0 equiv) and $K[B(C_6F_5)_4]$ (23 mg, 0.032 mmol, 2.2 equiv) in 1 mL of THF at room temperature with stirring. No color change was observed for the reaction mixture, but after 48 h of stirring at room temperature, volatiles were removed, and the crude material was triturated with 1 mL of hexane. The product was extracted with 3 mL of diethyl ether, filtered through Celite, concentrated to a volume of 0.5 mL, and cooled to −40 °C. The product was isolated as dark red crystals and dried *in vacuo* (7.8 mg, 0.0047 mmol, 32% yield). The IR spectrum of **2** prepared by this method was identical to that isolated by Method A above.

$(Cp^{iPr4})_2U(I)(CN^tBu)$ (3). A solution of ^{t}BuNC (22 μL, 0.19 mmol, 5.0 equiv) in 0.5 mL of hexane was added by pipette to a stirring solution of $(Cp^{iPr4})_2UI$ (32 mg, 0.039 mmol, 1.0 equiv) in 1 mL of hexane at room temperature. The reaction quickly changed from dark blue to dark yellow-green and was stirred for an additional 5 min at room temperature. Volatiles were removed *in vacuo*, then the product was extracted into 2 mL of pentane, filtered through Celite, concentrated to a volume of 0.5 mL, and cooled to −40 °C. The product was isolated as green crystals and dried *in* *vacuo* (30 mg, 0.033 mmol, 85% yield). X-ray quality crystals of **3** were grown from pentane at −40 °C. ^{1}H NMR (400 MHz, C_6D_6): δ 21.19 (broad), 16.53 (very broad), 12.63 (broad), 10.84 (broad), 4.37 (very broad), 0.23 (broad), −12.84 (s, FWHM = 16 Hz, CNC(C*H*$_3$)$_3$), −32.88 (broad), −42.57 (very broad), −59.47 (very broad). Assignments of numbers of hydrogen atoms were not possible due to the intrinsically broad nature of the signals (except for the ^{t}Bu group, which was much sharper) and the related difficulty of correcting the spectrum's baseline; $\mu_{\mathrm{eff}} = 3.22\ \mu_{\mathrm{B}}$ (298 K, Evans method, C_6D_6); IR: 2166 cm^{-1} (s, ν_{CN}), 1312 (w), 1295 (w), 1233 (w), 1198 (m), 1178 (m), 1145 (w), 1098 (w), 1055 (w), 981 (m), 949 (w), 919 (w), 844 (w), 778 (s), 696 (w), 668 (w), 615 (w), 582 (w), 538 (w), 521 (w). Anal. Calcd. (%) for $C_{39}H_{67}INU$ (**3**): C, 51.20; H, 7.38; N, 1.53. Found: C, 51.22; H, 7.29; N, 1.46.

Conflicts of Interest

There are no conflicts to declare.

Acknowledgments

This work was supported by the Director, Office of Science, Office of Basic Energy Sciences, Division of Chemical Sciences, Geosciences, and Biosciences Heavy Element Chemistry Program of the U.S. Department of Energy (DOE) at LBNL under Contract DE-AC02-05CH11231. M.A.B. acknowledges support from the National Science Foundation Graduate Research Fellowship Program under Grant No. DGE 1106400. S.H. thanks the Daimler and Benz Foundation (Grant No.: 32-06/17), the Fonds der chemischen Industrie (VCI), Paderborn University, and the University of Innsbruck for financial support. We thank College of Chemistry's NMR facility for resources provided and the staff for their assistance. Instruments in CoC-NMR are supported in part by NIH S10OD024998. We thank Dr. Steven Crossley for assistance with GC/MS measurements, I. Joseph Brackbill for helpful discussions, and Erik T. Ouellette for preparing the electrolyte for electrochemistry experiments.

Notes and References

[†] Electronic supplementary information (ESI) available: NMR spectra, UV-visible spectra, GC/MS experimental details, X-ray crystallography procedures and data tables, and electrochemical details and data. CCDC 2006480−2006482.

[#] We nevertheless thank a referee for suggesting this experiment and further note that the mechanism of metal-based reduction of isocyanides has been studied previously (see G. E. Niznik and H. M. Walborsky, *J. Org. Chem.*, 1978, **43**, 2396.)

[‡] It is possible that traces of $(Cp^{iPr4})_2UI$ may remain in solution and could also act as a source of iodide.

[§] While also quite rare, linear metallocenes with divalent lanthanides have been observed (see H. Sitzmann, T. Dezember, O. Schmitt, F. Weber, G. Wolmershäuser and M. Ruck, *Z. Anorg. Allg. Chem.*, 2000, **626**, 2241 and C. A. Gould, K. R. McClain, J. M. Yu, T. J. Groshens, F. Furche, B. G. Harvey and J. R. Long, *J. Am. Chem. Soc.*, 2019, **141**, 12967.)

[§§] Using 6-coordinate U(III) and 7-coordinate U(IV) to approximate both the change in oxidation state and coordination number between **2** and **3**, a difference of 0.075 Å is predicted (see R. D. Shannon, *Acta Crystallogr., Sect. A: Cryst. Phys., Diffr., Theor. Gen. Crystallogr.*, 1976, **32**, 751.)

1 S. T. Liddle, *Angew. Chem., Int. Ed.*, 2015, **54**, 8604.

2 M. J. Monreal, R. K. Thomson, T. Cantat, N. E. Travia, B. L. Scott and J. L. Kiplinger, *Organometallics*, 2011, **30**, 2031.

3 D. L. Clark, A. P. Sattelberger, S. G. Bott and R. N. Vrtis, *Inorg. Chem.*, 1989, **28**, 1771.

4 L. R. Avens, S. G. Bott, D. L. Clark, A. P. Sattelberger, J. G. Watkin and B. D. Zwick, *Inorg. Chem.*, 1994, **33**, 2248.

5 C. D. Carmichael, N. A. Jones and P. L. Arnold, *Inorg. Chem.*, 2008, **47**, 8577.

6 W. J. Evans, S. A. Kozimor, J. W. Ziller, A. A. Fagin and M. N. Bochkarev, *Inorg. Chem.*, 2005, **44**, 3993.

7 H. S. La Pierre, F. W. Heinemann and K. Meyer, *Chem. Commun.*, 2014, **50**, 3962.

8 P. L. Arnold, *Chem. Commun.*, 2011, **47**, 9005.

9 M. Ephritikhine, *Dalton Trans.*, 2006, 2501.

10 A. R. Fox, S. C. Bart, K. Meyer and C. C. Cummins, *Nature*, 2008, **455**, 341.

11 W. J. Evans and S. A. Kozimor, *Coord. Chem. Rev.*, 2006, **250**, 911.

12 M. Ephritikhine, *Organometallics*, 2013, **32**, 2464.

13 F. A. Cotton, G. Wilkinson, C. A. Murillo and M. Bochmann, *Advanced Inorganic Chemistry,* 6th ed, John Wiley & Sons, Inc., New York, 1999.

14 M. Sharma and M. S. Eisen, *Struct. Bonding (Berlin, Ger.)*, 2008, **127**, 1.

15 W. J. Evans, G. W. Nyce, K. J. Forrestal and J. W. Ziller, *Organometallics*, 2002, **21**, 1050.

16 W. J. Evans, S. A. Kozimor, W. R. Hillman and J. W. Ziller, *Organometallics*, 2005, **24**, 4676.

17 N. A. Siladke, J. W. Ziller and W. J. Evans, *Z. Anorg. Allg. Chem.*, 2010, **636**, 2347.

18 N. Tsoureas, A. F. R. Kilpatrick, O. T. Summerscales, J. F. Nixon, F. G. N. Cloke and P. B. Hitchcock, *Eur. J. Inorg. Chem.*, 2013, **2013**, 4085.

19 C. J. Windorff and W. J. Evans, *Organometallics*, 2014, **33**, 3786.

20 W. J. Evans, S. A. Kozimor and J. W. Ziller, *Chem. Commun.*, 2005, 4681.

21 W. J. Evans, S. A. Kozimor, J. W. Ziller and N. Kaltsoyannis, *J. Am. Chem. Soc.*, 2004, **126**, 14533.

22 W. J. Evans, S. A. Kozimor and J. W. Ziller, *Science*, 2005, **309**, 1835.

23 W. J. Evans, K. A. Miller, W. R. Hillman and J. W. Ziller, *J. Organomet. Chem.*, 2007, **692**, 3649.

24 W. J. Evans, E. Montalvo, J. W. Ziller, A. G. DiPasquale and A. L. Rheingold, *Inorg. Chem.*, 2010, **49**, 222.

25 C. L. Webster, J. W. Ziller and W. J. Evans, *Organometallics*, 2012, **31**, 7191.

26 C. L. Webster, J. E. Bates, M. Fang, J. W. Ziller, F. Furche and W. J. Evans, *Inorg. Chem.*, 2013, **52**, 3565.

27 C. L. Webster, J. W. Ziller and W. J. Evans, *Organometallics*, 2013, **32**, 4820.

28 F.-S. Guo, Y.-C. Chen, M.-L. Tong, A. Mansikkamäki and R. A. Layfield, *Angew. Chem., Int. Ed.*, 2019, **58**, 10163.

29 M. A. Boreen, D. J. Lussier, B. A. Skeel, T. D. Lohrey, F. A. Watt, D. K. Shuh, J. R. Long, S. Hohloch and J. Arnold, *Inorg. Chem.*, 2019, **58**, 16629.

30 M. A. Boreen, G. Rao, D. G. Villarreal, F. A. Watt, R. D. Britt, S. Hohloch and J. Arnold, *Chem. Commun.*, 2020, **56**, 4535.

31 M. A. Boreen, K. N. McCabe, T. D. Lohrey, F. A. Watt, L. Maron, S. Hohloch and J. Arnold, *Inorg. Chem.*, 2020, **59**, 8580.

32 J. Maynadié, J.-C. Berthet, P. Thuéry and M. Ephritikhine, *J. Am. Chem. Soc.*, 2006, **128**, 1082.

33 J. Maynadié, J.-C. Berthet, P. Thuéry and M. Ephritikhine, *Organometallics*, 2006, **25**, 5603.

34 R. R. Langeslay, C. J. Windorff, M. T. Dumas, J. W. Ziller and W. J. Evans,

Organometallics, 2018, **37**, 454.

35 S. J. Connelly, W. Kaminsky and D. M. Heinekey, *Organometallics*, 2013, **32**, 7478.

36 F. Weber, H. Sitzmann, M. Schultz, C. D. Sofield and R. A. Andersen, *Organometallics*, 2002, **21**, 3139.

37 J. Maynadié, N. Barros, J.-C. Berthet, P. Thuéry, L. Maron and M. Ephritikhine, *Angew. Chem., Int. Ed.*, 2007, **46**, 2010.

38 F.-S. Guo, N. Tsoureas, G.-Z. Huang, M.-L. Tong, A. Mansikkamäki and R. A. Layfield, *Angew. Chem., Int. Ed.*, 2020, **59**, 2299.

39 I. Ugi and R. Meyr, *Chem. Ber.*, 1960, **93**, 239.

40 N. Tsoureas, A. F. R. Kilpatrick, C. J. Inman and F. G. N. Cloke, *Chem. Sci.*, 2016, **7**, 4624.

41 K. Nakamoto, *Infrared and Raman Spectra of Inorganic and Coordination Compounds: Part B: Applications in Coordination, Organometallic, and Bioinorganic Chemistry*, 6th ed, John Wiley & Sons, Inc., Hoboken, New Jersey, 2009.

42 F. A. Cotton and F. Zingales, *J. Am. Chem. Soc.*, 1961, **83**, 351.

43 W. W. Lukens, M. Speldrich, P. Yang, T. J. Duignan, J. Autschbach and P. Kögerler, *Dalton Trans.*, 2016, **45**, 11508.

44 M. del Mar Conejo, J. S. Parry, E. Carmona, M. Schultz, J. G. Brennann, S. M. Beshouri, R. A. Andersen, R. D. Rogers, S. Coles and M. B. Hursthouse, *Chem. - Eur. J.*, 1999, **5**, 3000.

45 W. J. Evans, T. J. Mueller and J. W. Ziller, *Chem. - Eur. J.*, 2010, **16**, 964.

46 C. Boisson, J.-C. Berthet, M. Lance, M. Nierlich and M. Ephritikhine, *J. Organomet. Chem.*, 1997, **548**, 9.

47 P. Rungthanaphatsophon, O. Jonathan Fajen, S. P. Kelley and J. R. Walensky, *Inorganics*,

2019, **7**, 105.

48 N. G. Connelly and W. E. Geiger, *Chem. Rev.*, 1996, **96**, 877.

49 A. C. Brown, A. B. Altman, T. D. Lohrey, S. Hohloch and J. Arnold, *Chem. Sci.*, 2017, **8**, 5153.

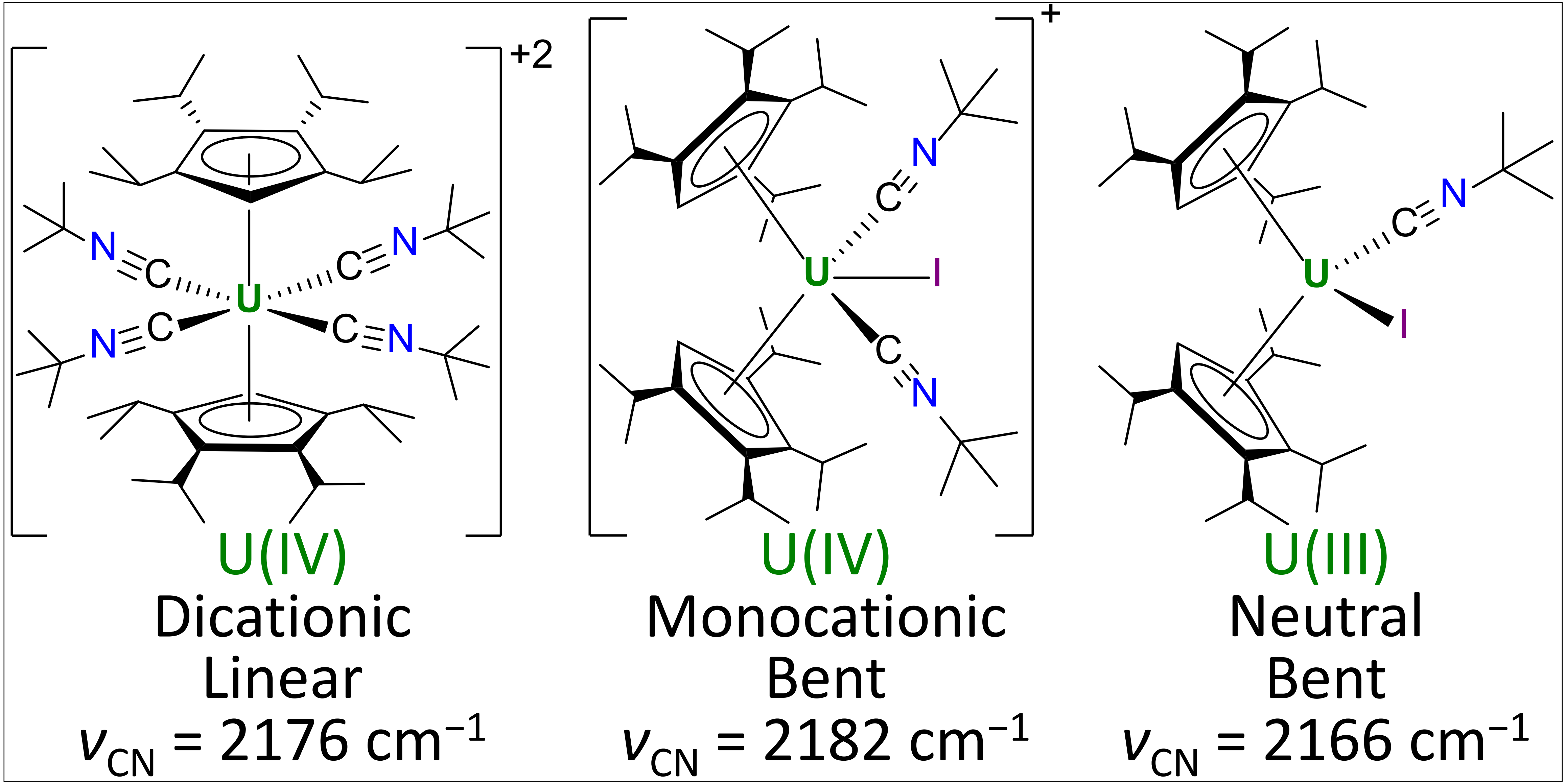

One sentence highlight: Reactions of uranium(III) metallocenium salt $[(Cp^{iPr4})_2U][B(C_6F_5)_4]$ with *tert*-butyl isocyanide yielded cationic uranium(IV) products, including a rare example of a linear f-block metallocene complex.